Pure Appl. Chem., Vol. 78, No. 3, pp. 525–539, 2006.
doi:10.1351/pac200678030525

INTERNATIONAL UNION OF PURE AND APPLIED CHEMISTRY

HOW TO ACCESS STRUCTURE AND DYNAMICS OF SOLUTIONS: THE CAPABILITIES OF COMPUTATIONAL METHODS

(Special Topic Article)

BERND M. RODE‡ AND THOMAS S. HOFER

Theoretical Chemistry Division, Institute of General, Inorganic and Theoretical Chemistry, University of Innsbruck, Innrain 52a, A-6020, Innsbruck, Austria

‡Corresponding author: Tel.: +43-512-507-5160; Fax: +43-512-507-2714; E-mail: Bernd.M.Rode@uibk.ac.at

How to access structure and dynamics of solutions: The capabilities of computational methods

(Special Topic Article)

Abstract: The progress of computational chemistry in the treatment of liquid systems is outlined, and the combination of the statistical methods (Monte Carlo, MC, and molecular dynamics, MD) with quantum mechanics as the main foundation of this progress is emphasized. The difficulties of experimental studies of liquid systems without having obtained sophisticated theoretical models describing the structural entities and the dynamical behavior of these liquids demonstrate that chemistry research is in a transition phase, where theory and high-performance computing have not only become a valuable supplement, but an essential and almost indispensable component to secure a correct interpretation of measured data.

Keywords: statistical simulations; structure of liquids; picosecond dynamics; ab initio simulation methods; QM/MM simulations; QMCF/MD simulations.

INTRODUCTION

Every experimental result is—at the best—as good as the theoretical model employed for its interpretation. Whenever reading new results obtained by any of today's sophisticated experimental methods, in particular spectroscopy, one should keep in mind that usually there is a quite complicated way from the actually measured data to the final results, e.g., the determination of a structure: A theoretical model has to be defined, to which the measured data are fitted until the "best possible" agreement is achieved, mostly within a few percent of deviation. While this is still not too error-prone in the case of highly regular solids, in the case of gases with their high mobility of components, this procedure becomes more difficult, and in the liquid state, where this high mobility is combined with a density similar to solids, any a priori postulated models can be much too simplified approximations, if not at all wrong.

Therefore, the quality of theoretical models plays a pivotal role in the determination of structural parameters, and even more, when other physicochemical phenomena such as reaction dynamics and mechanisms (where all interpretation of measurements depends on a correct structural model plus corresponding mechanistic models) are evaluated.

In principle, quantum mechanics provide a general theory for chemical processes at a molecular level, but the corresponding methods, based on numerical solutions of the Schrödinger equation [1] at various levels of accuracy (and approximations), are subject of severe technical limitations even with today's best computational facilities, and the model systems accessible by ab initio calculations usually reflect the situation at 0 K in the gas phase and are mostly also much too small to be representative for the bulk of a liquid.

On the other hand, it has been repeatedly shown that the classical methods established in the treatment of liquid systems in the form of statistical Monte Carlo (MC) and molecular dynamics (MD) simulations, are not sufficiently accurate whenever n-body effects, polarization, and charge transfer play a crucial role for structure and dynamics of the system under investigation [2–6]. In such cases, classical simulations are usually adapted by the use of numerous different, more or less empirically generated model potentials, e.g., polarizable models [7–9] and functions fitted to reproduce certain experimental data. In these cases, there is no guarantee of the physical meaningfulness of such models, in particular,

as these model potentials usually reproduce only a subset of experimentally observed data, while failing in the prediction of other properties.

The straightforward answer to these problems would be the application of quantum mechanics for the evaluation of energies (MC) and forces (MD) in the statistical procedures, which can reproduce the liquid state of a bulk at a given temperature within their formalism of periodic boundary conditions, minimal image convention, and temperature-controlling algorithms [10] (e.g., Metropolis in the case of MC [11], Berendsen in the case of MD [12]). A short consideration of the number of configurations (MC) or time steps (MD) usually needed for equilibration and representative sampling and the computational effort needed for the corresponding number of quantum mechanical (QM) calculations of energies or gradients quickly reveals that this approach leads to unmanageable dimensions, at least for a physically reasonable size of the elementary box of the simulations, necessary to be representative for a liquid system.

METHODOLOGIES FOR SIMULATING LIQUID SYSTEMS

Solutions for the aforementioned dilemma were sought in different ways: One principle possibility is the reduction of the quantum chemical accuracy from nonempirical ab initio level to semiempirical molecular orbital (MO) or density functional theory (DFT) methods, which, however, still requires a simultaneous reduction of the system size to 30–60 molecules. The second approach retains the accuracy of nonempirical ab initio methods at Hartree–Fock (HF) or even better level, but only for a subsystem of particular importance and interest, while describing the rest of the box with several hundred solvent molecules by classical molecular mechanics (MM) [13–16]. The latter approach has become known under the name of QM/MM simulations and will be discussed in more detail hereafter.

Retreating to semiempirical MO procedures such as AM1 [17] or PM3 [18] proved impracticable even for simple solvated ions, and even strongly simplified basis sets like STO-3G in ab initio methods gave very unsatisfactory results [19]. The use of density functional methods appeared much more promising, and molecular dynamics of molecular clusters with 30 to 60 molecules, using the BLYP functional [20,21] for the evaluation of forces have become a quite popular instrument since their introduction by Car and Parrinello [22]. In the past few years, however, it was found that the BLYP functional is not very suitable for treating solutes in hydrogen-bonding solvents, leading to too rigid structures and even wrong coordination numbers [3,4,23,24]. The same is true for other simple DFT methods such as RIDFT [25], but the hybrid functional B3LYP [26] appears much more suitable for reproducing the structure of liquids and solutions [25,27,28], although still overemphasizing rigidity and thus leading to too slow dynamics. Besides that, the computational effort for B3LYP calculations is virtually the same as that of ab initio HF-level calculations with the same basis set, and thus the speed advantage of the DFT methods vanishes.

Under these circumstances, the QM/MM approach is the most practicable way presently, employing a sufficiently large simulation box on the one hand, and on the other hand preserving sufficient accuracy for the relevant subregion of the system. It should not be concealed at this point that this selection of a "relevant" subregion implies restrictions for the chemical systems treatable: An increasing size of the subsystem leads to an exponential increase of the computational effort, and concentrated solutions, where the solute(s) are located all over the solution, call for further methodical compromises and developments. A further obstacle for a widespread application of ab initio QM/MM simulations is their actual computational demand. The necessary number of configurations (MC) or time steps (MD) boosts the number of ab initio calculations in one simulation to 50 000, sometimes even more than 100 000. Even with a modest basis set (DZP is a good compromise between speed and accuracy) and parallel processing, the simulation time amounts to several months, 95 to 98 % of it being spent on the QM calculations. The constantly increasing speed of computers and their availability at constantly decreasing prices allows quite some optimism, however, that the applicability of these methods will quickly improve and that increasingly complex system can be studied at this level of accuracy.

If performed at a sufficient level of accuracy, simulations can supply a highly rewarding variety of valuable information, which would have required expensive and tedious experimental settings or, in many cases, is not yet accessible with present experimental methods. The latter is particularly true for liquid systems with ultrafast dynamics, i.e., in the pico- or even femtosecond range [3,4,29]. Besides structural data accessible through radial and angular distribution functions, the simultaneous presence of different complex species, often interchanging within picoseconds, can be detected, thus creating a suitable model setting for the interpretation of spectrosopic data. Detailed vibrational spectra can be evaluated, especially for the solute and its immediate environment, by Fourier transformation of the velocity autocorrelation functions, and the kinetics of complexes in solution can be analyzed by quantum chemical model calculations and simulations [30] via ligand mean residence times (MRTs) [29] and the determination of ligand-exchange constants [31]. The importance of simulations becomes striking when these processes occur on a time scale below 10^{-9} s, where NMR methods reach the limits of their capability and femtosecond laser pulse spectroscopy does not yet provide suitable settings for the composite systems to be studied.

One of the main features, where simulations are really superior to experimental work, is the possibility of easily evaluating any kind of atom–atom pair distribution. In more complex systems (e.g., mixed solvents and solutions simultaneously containing several solute species), this is an enormous advantage over spectrosopic approaches, where only averaged data (e.g., atom–atom distances) can be "seen". Even sophisticated (and expensive!) techniques such as neutron diffraction with isotope substitution (NDIS) [32,33] can only partly overcome the problem of many overlaying distribution functions. An example of this problem is shown in Fig. 1 (see p. 531), illustrating the overlay of various atom–atom radial distribution functions (RDFs) for Ca(II) ion in aqueous ammonia [34]. It is evident that an analysis of a sum of all these solute–solvent and solvent–solvent RDFs as visible in X-ray or neutron diffraction measurements, could be very ambiguous and hardly be correctly interpreted without having a simulation result to build a suitable model for fitting.

AB INITIO QM/MM MD SIMULATIONS: PRINCIPLES AND APPLICATIONS

In order to avoid artificial symmetry effects and to include all solvation shells plus the effects of surrounding bulk, the basic simulation box should contain several hundred solvent molecules. To treat such a box completely by means of ab initio quantum mechanics is still far beyond any available computational capacities. The QM/MM compromise leading to feasible computational requirements, but still maintaining the desired accuracy, is to apply the QM formalism to the most chemically important region of the system, and to retain the description by classical MM for the remaining part of it. This idea, originally proposed for the treatment of larger biomolecules, has been successfully applied to solvated ions in the past decade [3,4,35].

In such ab initio QM/MM simulations of solvated ions, the basic box is partitioned into an inner region containing the ion plus one or two complete solvation shells (QM region), where all forces are usually calculated at HF level with double zeta basis sets plus polarization functions, which has been shown to be the best compromise between accuracy and computational effort. For heavier ions, the inner electrons are considered by—eventually relativistically corrected—effective core potentials (ECPs). The remaining system (MM region), typically containing around 500 solvent molecules, is treated by classical MM employing ab initio generated (with identical basis sets) pair and three-body potentials as in classical simulations. Many-body effects in this region could also be treated by polarizable pair potential functions or related methods [7–9,36].

The necessary size of the QM region varies with the number of solvent ligands attached to the ion and can be estimated from an initial classical simulation. The use of this approach requires a smoothing procedure in the transition region between QM and MM regions, which allows transitions of solvent molecules without discontinuities, and the employment of a flexible solvent model in the MM re-

gion such as the BJH-CF2 model [37,38], compatible with the full flexibility of the molecules in the QM region. Such flexible model potentials always contain, in addition to the intermolecular term, an intramolecular term.

This flexibility, which allows explicit hydrogen movements, also demands an appropriate short time step in the MD simulation, usually 0.2 fs. This requirement leads to a total amount of 50 000 steps for an MD simulation of just 10 ps, which explains the enormous computational effort of QM/MM simulations, despite the reduction of the QM formalism to a smaller inner part of the system. One step of the simulation with the evaluation of quantum mechanically calculated forces requires a few minutes of CPU time on 4–10 processors (Intel 2400/2800 MHz), thus generating a total computation time of 30 to 300 days per simulation, most of this time being dedicated to the QM calculations. This also implies that the parallelization of the computations has its limits in the parallelizability of the QM code (integrals, diagonalization). With the parallel TURBOMOLE program [39–42] employed in our simulations and the aforementioned basis sets, the optimal number of processors lies between 4 and 10, according to the number of ligands located in the solvation shell(s).

The MD simulation protocol of such simulations normally refers to one ion immersed in 200–500 solvent molecules in a cubic box of the experimental density. The QM region includes the full first, sometimes also the second hydration sphere, and solvent molecules are allowed to enter/leave the QM region through a transition region of 0.2 Å width, ensuring a smooth transition between QM and MM forces. Periodic boundary conditions are applied, and long-range interactions are handled by the reaction field method. The temperature of the NVT ensembles (constant number of particles N, constant volume V, constant temperature T) is controlled by the Berendsen algorithm [12]. For water, the aforementioned BJH-CF2 model [37,38] is preferably used, as it allows explicit hydrogen movements (which, on the other hand, request the time step of 0.2 fs for the simulations). The preference of this water model over others is founded on its flexibility, allowing intramolecular vibrations and relaxation processes and thus the evaluation of vibrational spectra of the ligand molecules and on its facilitation of smoother transitions from the QM region (where all ligands are fully flexible) to the MM region. The pair and three-body potential functions required for the MM region of the simulations are constructed from the respective energy surfaces, ab initio calculated with the same basis sets used in the QM/MM MD simulations, and fitted to analytical potential functions.

As already mentioned, the accuracy of a simulation is a very crucial point, especially when data exceeding the reach of experimental confirmation are to be evaluated. Therefore, any simulation method has to be tested with some systems, where a good comparability with suitable experiment is given. In the case of structure and ultrafast dynamics, the solvent water is such a crucial test system, where all kinds of experimental methods have been employed to determine the structural features of the liquid and where femtosecond laser pulse spectrosopy has already provided reliable data on dynamics, e.g., the life time of hydrogen bonds of ~0.5 ps [43]. In ab initio simulations of solvated ions [3,4], good agreement of the results with most of the available experimental data was found, and in some cases of deviation this discrepancy may as well suggest the use of better models for the interpretation of the experimental measurements. The use of MOLVISION, the new visualization tool for simulation trajectories [44], has produced a number of video clips illustrating the manifold dynamic processes and interchange between structural entities occurring in solutions of ions and have been made accessible on the Web (<www.molvision.com>, video clips).

THEORETICAL MODELS AND EVALUATION OF EXPERIMENTS: THE CRUCIAL INTERDEPENDENCE

This section will, on the one hand, point out the importance of highly accurate experimental data for the assessment of a simulation's quality and, on the other hand, demonstrate the limitations of common simple chemical models for complexes in solution and thus the need for sophisticated and accurate sim-

ulations in order to interpret spectroscopic data and to properly deal with structure and dynamics in solution.

For the first item, the treatment of the most prominent and important solvent, water, serves as the most suitable paradigm. The enormous amount of literature on water models and on simulations of liquid water [45–47] proves that up to now this is a subject of continuous actuality and probably the best-investigated system to evaluate theoretical approaches with respect to their ability to reproduce macroscopic and microscopic properties obtained by increasingly accurate and sophisticated experimental methods. Already, very early MC simulations with relatively simple potential models [48,49] had indicated that pair potentials might not be appropriate to correctly describe liquid water. The need to incorporate higher n-body potentials in simulations has been multiply proven to be even more essential in the case of solvated ions [2–4,50]. However, even the direct or indirect implementation of n-body interactions aiming at the inclusion of polarization and charge-transfer effects (SPC/E, etc.) did not yet lead to more than a satisfactory description of a part of data, while missing reproducing others. Therefore, the quality of the simulations had to be improved by the inclusion of QM effects, introduced by the previously mentioned Car–Parrinello and ab initio QM/MM methods. The most critical experimental data to measure the quality of the theoretical approach were the number [51,52] of H bonds and their lifetime, determined by femtosecond laser pulse spectroscopy [43]. The most recent experiments had indicated—in contrast to all previous models based on a flexible ice-like structure with 4 hydrogen bonds binding each water to its surrounding neighbors—that each water molecule in the liquid at room temperature forms only 2 strong H bonds. These are supplemented by some considerably weaker bonds and thus an average number of H bonds of 2.8 results. The lifetime of these H bonds at room temperature was experimentally determined as 0.5 ps.

These data were only reproduced by recent ab initio QM/MM MD simulations at HF level with double-zeta plus polarization basis sets and the inclusion of two complete water shells around a central water into the quantum mechanically described part of the system [53], proving thus the crucial importance of quantum effects on the one hand and a suitable statistical mechanical formalism to achieve the necessary quality for an accurate description of the microscopic structure and the ultrafast dynamics of liquid water. This test of the method also included ab initio MP/2 [54] as well as B3LYP [28,55,56] DFT QM/MM MD simulations, proving that the influence of electron correlation is less important than the inclusion of quantum effects of a larger subsystem, and that DFT methods do not describe H bonds adequately [28,53,55,56].

The good achievement of the ab initio HF QM/MM MD simulation in this crucial test case lends a strong credibility to the reliability of data obtained by the same methodology for more complex systems like solvated ions. Such ions, however, can have a strong influence on the H-bond structure of the solvent, as shown by Soper and Leberman [57], who investigated the influence of high salt concentrations on the H-bond network of water and concluded that higher ionic concentrations have a similar effect as pressures of ~1 kbar. Microscopic properties and exchange dynamics for a number of these ions are not yet accessible by the same accurate experimental methods as for the solvent itself, and hence simulations are the only means for a detailed analysis of structure and dynamics at present. The results of these simulations give manifold indications that for many ions the common models based on a more or less regular and unique hydrate complex do not reflect the reality prevailing in solution and will thus not form an appropriate basis for the interpretation of experimental, in particular, spectroscopic data. This finding will be exemplified in the following, using simulation results for a variety of ions.

The well-known Jahn–Teller distortion of octahedral complexes with d^1 or d^9 electron configuration of the central ion as predicted by the ligand field model [58] is a first example in this context. In the case of Cu(II), the strength of this effect has even provoked some discussion about the coordination number, which is dominantly accepted as 6 [59–61], but some experimental data could also be fitted to a five-fold coordination as predicted by CP MD [23]. The rapid exchange of ligands ($k_{ex} = 10^{-9}$ s) and the associated fluctuation of ligand binding has already been discussed as a possible reason for this ambiguity [62].

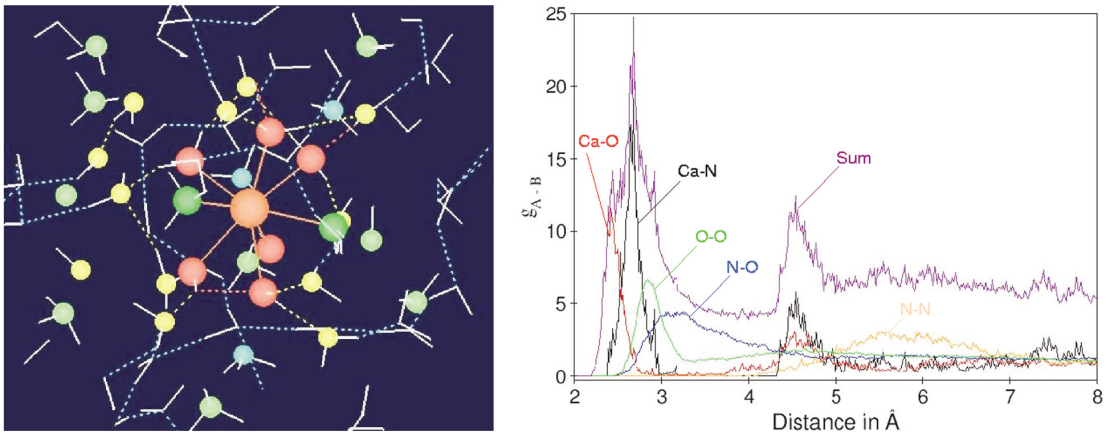

Fig. 1 Ca(II) in 18.6 % aqueous ammonia solution: Snapshot of the solvated ion (left side) and solute–solvent and solvent–solvent atom pair RDFs (right side).

The experimental investigations have proven that the Jahn–Teller effect is rather a strongly dynamical one [63], however, the time scale of these dynamics is clearly beyond the capability of the NMR method (10^{-9} s): Ab initio QM/MM simulations of Cu(II) and Ti(III) ion in water have shown that the Jahn–Teller distortions occur on the femtosecond scale [56,59,64], and that besides the classical structure with two opposite ligands at elongated distances other structures with three or four ligands at different bond lengths are also formed. On the other hand, the time-averaged magnitude of the distortions accessible via diffraction experiments [65] is in excellent agreement with the corresponding values from the simulations' RDFs [56,64], thus confirming once more the reliability of the simulations. It has to be mentioned, however, that it proved essential in the case of Jahn–Teller distorted ions to include the full second hydration sphere into the quantum mechanically described subsystem in order to achieve this agreement [56,64].

Sn(II) and Pb(II) in aqueous solution are main group ions, where distortions of the hydrates occur, leading to quite complicated structures in which different bond lengths occur [66,67] (cf. Fig. 3a). These peculiar structures also influence the dynamics of ligand exchange; in particular, the fast exchange of first-shell ligands of Sn(II) occurring on the picosecond scale is associated with the existance of weaker binding of some ligands [66]. Figure 2 illustrates the hydrate structure and the exchange processes between first and second hydration shell on the picosecond scale.

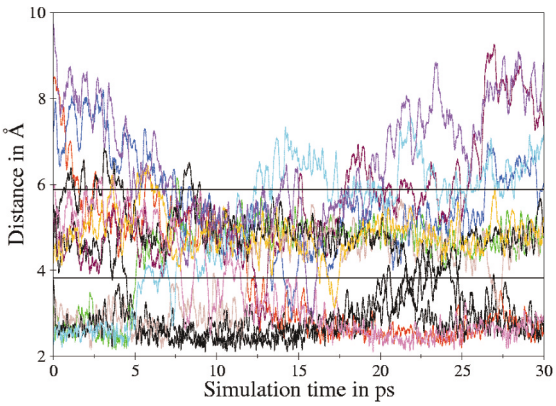

Fig. 2 Sn(II)–O distance plot showing water ligand migration between first and second hydration shell.

Even extremely stable hydrate complexes such as that of Cr(III) cannot be treated purely classically [68] or assumed to be rigid [69]. However, the treatment of first-shell water molecules by means of a separate interaction potential yields an improved description of the structure [70]. QM/MM MD simulations revealed very strong first-shell dynamics, where the associated distortions—although not leading to exchange processes—exert a strong influence on composition, structure, and dynamics of the second hydration shell [68]. A similar situation was found in the case of the trivalent main group metal ion Al(III) [71–74] (cf. Fig. 3).

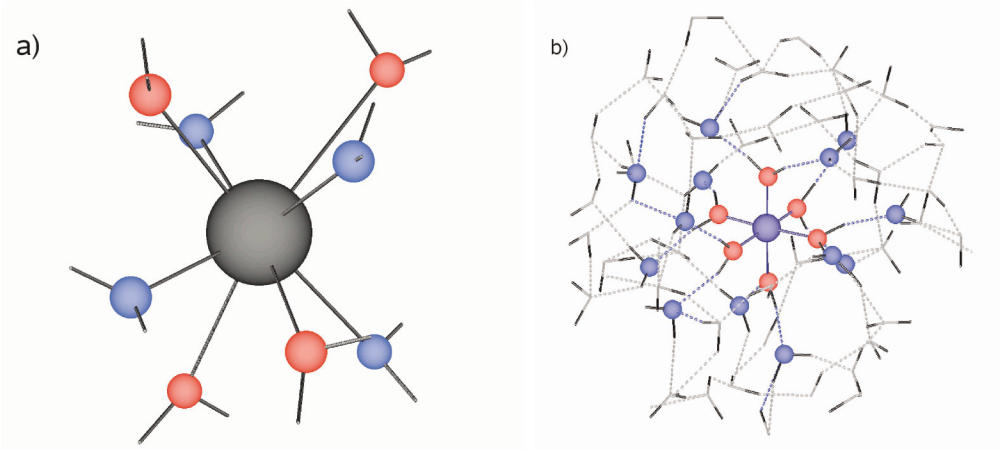

Fig. 3 (a) Sn(II) hydrate—within the first shell structure ligands with different bond lengths have been identified; (b) Al(III) hydrate—the kinetically inert first shell has a significant influence on the structure of the second shell.

The most striking examples for the inadequacy of simple and unique solvate complex models, however, are ions with ultrafast exchange dynamics: In these cases, numerous structures with a different number of ligands and thus a different structure coexist. Figure 4 illustrates Ag(I) hydrates [75] which are formed by the same ion within a time span of a few picoseconds. The dynamics can be monitored on a video clip of the supporting material. Cs(I) [29,55] and K(I) [76,77] are other typical ions, where numerous coordination numbers of the first shell coexist.

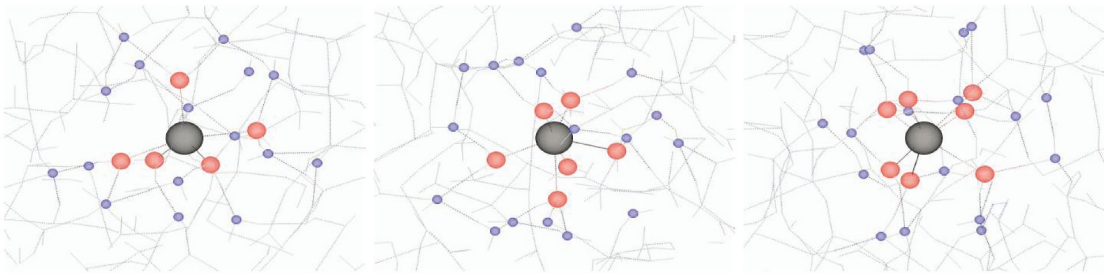

Fig. 4 Ag(I) hydrates interchanging within the picosecond scale obtained from a QM/MM MD simulation. (Red spheres indicate first-shell oxygens; second-shell oxygens are depicted in blue.)

This simultaneous presence of different hydrate complexes is not restricted to monovalent metal cations. Hg(II) is present in at least two different species [78], and Ba(II) [67] and Sn(II) [66] are examples of main group metal ions, where due to the lability of the first hydration shell and its specific

structural features, more than one complex species are present within the time span of every presently applicable spectroscopic technique.

The multispecies presence of solvate complexes, which is also found for other ligands, e.g., ammonia [79,80], has to be considered not only in the case of structural investigations by diffraction methods, but also in the discussion of ligand-exchange dynamics. Ligand-exchange reactions are commonly classified according to Langham and Gray [81] as either "associative" (A), "dissociative" (D), or "interchange" (I), according to the structure of the transition state in these hypothetical mechanisms. The activation volume measured by NMR [82,83] is employed to experimentally decide which type of mechanism dominates for a specific ion. It is obvious that the model underlying this interpretation, consisting of a single, unique hydrate complex and a single transition state for the ligand exchange, becomes obsolete whenever the ion is present in several complex species with different coordination numbers. The same is true for QM model calculations of ion–ligand clusters and the corresponding transition states, even if the gas-phase calculations consider the solvent influence by simple models such as polarizable continuum model (PCM) [84] and introduce temperature by a statistical mechanics procedure. Such calculations, frequently employed to determine exchange mechanisms [85], are definitely a too simplistic approach, whenever multiple species are involved in exchange processes. In such cases, simulations of the liquid systems with a detailed species analysis and observation of actually occurring exchange processes, including the determination of their reaction constants, are the only adequate theoretical treatment.

The presence of more than one ligand type binding to a central ion or molecule leads to an even more complicated situation. The previously given example of Ca(II) in aqueous ammonia (Fig. 1) not only illustrates the difficulties of obtaining a correct experimental result for the average structure of the ion solvate, which in this case contains both water and ammonia ligands. A further analysis of the simulation shows that a mixture of several solvates of the type $[Ca(NH_3)_m(H_2O)_n]^{2+}$ "hides" behind the average composition. Therefore, also the exchange dynamics of ligands at the central ion are a quite complicated process involving a number of species, and the only way to characterize these dynamics is a determination of the MRTs of ligands in the first solvation shell (supplying also the mean exchange rate constants for both ligands) and the consideration of the relative contribution of all species present in the solution in the mechanism(s) of ligand exchange.

Even if one of the ligands exchanges at a much slower time scale than the other, the situation remains complicated enough, as can be exemplified in the cases of Cu(II) and Ni(II) amine complexes $[M(NH_3)_m]^{2+}$, m being a value between 0 and 4. In the case of Cu(II), where the exchange of water ligands occurs much faster than in hydrates of other transition-metal ions due to the Jahn–Teller effect and the associated elongated ion–ligand bonds [56,60,82], the presence of ammonia ligands produces an even more distorted structure and thus—together with electronic effects—enhances the rate of exchange. With two ammonia ligands located at the Cu(II) ion, the water exchange rate constant is lowered to an order of magnitude of 10^{-11}, and several $[Cu(NH_3)_2(H2O)_n]^{2+}$ species contribute to the exchange mechanism [86]. In the case of Ni(II), whose exchange rate of water ligands is in the order of 10^{-5} [82] due to the absence of the Jahn–Teller effects, ammonia ligands produce distortions of the solvate structure, which, together with electronic effects, enhance again the exchange rate of water ligands [87]. In this case, however, more than two ammonia ligands are needed to reduce the MRT of water molecules in the first shell to the picosecond range [87]. Again, several species of the solvated complex are present, and the exchange mechanism involves all of them.

Most metal ions form a distinct second hydration shell, and the ligands of this shell exchange extremely fast with the bulk (a third hydration shell is rarely found), making an experimental determination of these processes very difficult or even impossible with present means. On the other hand, these ultrafast dynamics facilitate their study by ab initio QM/MM MD simulations, where 20–30 ps simulation time presently requires several months on a multiprocessor high-performance computer, thus still limiting the study of exchange processes to the picosecond range.

Table 1 lists MRTs of ligands in first and second hydration shell in picoseconds, determined by ab initio QM/MM MD simulations for a number of ions, and the species distribution for these shells.

Table 1 Mean ligand residence time τ in ps and occurring coordination numbers CN in first and second shell obtained from QM/MM MD simulations. (Detailed comparison of the QM/MM results with data from other simulations and experimental work are given in the references listed with the respective ions.)

	First shell		Second shell		
Ion	τ_1	CN_1	τ_2	CN_2	Refs.
Li(I)[a]	–	3–5	–	–	[88]
Na(I)[a]	2.4	4–7	–	–	[76,77]
K(I)[a]	2.0	6–9	–	–	[76,77]
Rb(I)[a]	2.0	4–11	–	–	[89]
Cs(I)[a]	1.5	5–10	–	–	[29,55]
Ag(I)[a]	5.5	4–7	2.6	13–23	[29,75]
Au(I)[a]	3.1	4–8	4.6	26–37	[29,90]
Mg(II)[a]	NA	6	–	10–14	[91]
Mg(II)[b]	NA	6	4.3	–	[92]
Ca(II)[a]	>43	7–8	4.4	16–23	[28,29]
Sr(II)[a]	45	8–10	6.1	17–28	[93]
Ba(II)[a]	19	8–11	5.5	19–29	[94]
Sn(II)[a]	5.0	6–10	3.8	19–29	[66]
Pb(II)[a]	NA	9	5.6	20–30	[67]
V(II)[a]	NA	6	7.5	13–19	[29,95]
Mn(II)[a]	NA	6	6.8	11–19	[29,95]
Mn(II)[b]	NA	6	4.4	21–30	[93]
Fe(II)[a]	NA	6	5	10–14	[29,96]
Co(II)[a]	NA	6	6.8	11–19	[29,97]
Ni(II)[a]	NA	6	8.0	10–16	[87]
Cu(II)[a]	NA	6	7.7	9–15	[29,56]
Cu(II)[b]	NA	6	3	10–16	[56]
Zn(II)[a]	NA	6	10.5	11–18	[98]
Zn(II)[b]	NA	6	3.3	10–18	[98]
Cd(II)[a]	NA	6	4.6	8–16	[99]
Hg(II)[a]	23.6	6–7	4.8	15–26	[29,78]
Al(III)[a]	NA	6	18.1	11–17	[71]
Al(III)[b]	NA	6	26.4	10–14	[71]
Tl(III)[a]	NA	6	12.8	15–22	[93]
Ti(III)[a]	NA	6	8	–	[64]
Ti(III)[b]	NA	6	37	10–12	[29,64]
Cr(III)[a]	NA	6	7.5	12–20	[29,68]
Co(III)[a]	NA	6	11	12–17	[29,100]
Fe(III)[a]	NA	6	19.8	11–16	[29,96]
La(III)[a]	>250	9–10	8.4	18–28	[93]

[a]One-shell QM/MM MD simulation.
[b]Two-shell QM/MM MD simulation.
NA: not accessable yet by ab initio QM/MM MD simulations.

Table 1 provides much insight into several aspects of the physicochemical behavior of the listed ions in aqueous solution: Wherever there is no unique coordination number, be it in the first or second shell, it is clear that exchange processes occur so fast that one has to expect at any time two or more hydrated species to be simultaneously present, thus requiring quite sophisticated models with species of different conformation and with different mean bond lengths and angles to fit any statistically averaged measured data such as diffraction patterns. At the same time, this has consequences for any assumed ligand-exchange mechanisms. Visualization of the associated trajectories (supporting materials, video clips) clearly shows that in such cases not a unique mechanism and no unique transition state determines how exchange processes take place, but that there are numerous possibilities, from which one could at the best assign a "preferred" or "dominant" character of these processes. Table 1 also explains why an experimental study of structure and dynamics of second hydration shells is a most difficult task, even for strongly hydrated trivalent ions, as all of the MRTs of second-shell ligands are in the picosecond range, and the coordination number distribution is very wide in all cases, corresponding to a number of quite different species with strongly varying arrangement of ligands. Finally, it has to be concluded, therefore, that a correct description of a hydrated ion has to take into account the full dynamics of first and second shell, thus making the results of static models, even those including solvent effects by implicit models [85] (such as PCM or COSMO [84]) a somewhat simplistic approach to the "real" situation in solution, although implicit solvent methods can reproduce some thermodynamic quantities (such as solvation energies) quite satisfactorily.

A comparison of the isoelectronic ions Cs(I), Ba(II), and La(III) strongly points at the need of a QM description of at least ion and first hydration shell, as there is no linear dependence of changes in MRTs and coordination number distributions from the formal charge of the ion, apparently due to a nonlinear behavior of ligand–ion charge transfer. The same nonlinear behavior is found for bond lengths and ion–ligand bond force constants. Only a QM treatment of the system can describe such charge-transfer effects completely and correctly.

All of these findings seem to give clear directions for future work related to solvated ions and short-lived complexes in solution: Joint operations by experimentalists and theoreticians appear mandatory, providing accurate measurements by various spectroscopic techniques and at the same time a clear picture from accurate simulations, which models are adequate for the interpretation of the measured data [101–104].

A large number of biological processes involving metal ions as hydrates or complexes takes place on the nano- or even picosecond scale. Their elucidation will require similar joint efforts by theoretical and experimental methods, thus making a further methodical development of simulation methods one of the most important tasks of computational chemistry.

FUTURE PERSPECTIVES

Even as ab initio QM/MM simulations have reached a stage of high accuracy and performance in the theoretical treatment of liquid systems, their range of applicability is still quite restricted due to inherent technical problems, thus calling for further significant methodical developments and improvements. One of the main obstacles for a wider applicability is how conventional QM/MM simulations take into account the QM forces as a kind of "correction" of an MM system. This formalism requires, besides the QM calculation of the interactions inside the QM region and the force-field calculations within the MM region, the evaluation of interactions between species inside and outside the QM region, which is usually achieved with the help of ab initio constructed pair and three-body potential functions. The construction of these functions is a time-consuming and tedious task, implying the evaluation of several thousands if not ten thousands of single points on the energy surfaces for all interacting species pairs and triples, followed by the search for suitable analytical functions representing these interactions [105]. This problem becomes the more stringent, the more complicated the solute is and the more different components it contains (e.g., in a mixed complex of a metal ion). On the other hand, it is just

these composite solutes that attract the most interest both in solution chemistry and in biological chemistry.

Seeing this dilemma, a new ab initio MD simulation method has been developed, which does not require the construction of any other potential functions except those for solvent–solvent interactions, maintains all the advantages of large simulation boxes and ensures the accuracy of ab initio quantum mechanics for all forces acting in the chemically most relevant region [106]. Interactions between solute and more distant solvent molecules are incorporated by a dynamically adjusted, quantum mechanically derived force field corresponding to the actual molecular configuration of the simulated system. This new formalism of "ab initio quantum mechanical charge field (QMCF)/MD simulations" achieves these goals by a moderate extension of the QM region to include the second solvent layer [106], as already found desirable in simulations of some ions in water [54,64,71,98], with a simultaneous use of quantum mechanically calculated data for the continuously changing charge distribution in the solute and its first surrounding solvent layer, and by the evaluation of all interactions of the solute with more distant solvent molecules on the basis of a dynamic charge field. First test simulations performed for some hydrated metal ions, for which high-quality conventional QM/MM MD simulations were already available, have proven not only equivalence but even superiority of the new procedure, and thus the way to ab initio QM/MM simulations of the aforementioned composite systems seems to be open.

Obviously, the extension of the QM region intensifies the "Scylla and Charybdis" problem of navigating between sufficient accuracy of the QM calculations and a prohibitively long computation time. The migration from 32- to 64-bit Opteron processors has already made this navigation much easier, and a simulation by the QMCF formalism does not take much more time now than a conventional ab initio QM/MM simulation with only one solvation layer took two years ago. Therefore, access to more complex systems seems to be not only feasible from the methodical point of view now, but also within the technical capacity of the near future.

CONCLUSION

Looking at the development of theoretical and computational chemistry, the field of chemical simulations can be valued as a particularly suitable example to demonstrate a general change in chemical sciences, somehow paralleling the development of physics in the dawn of the 20th century: At that time, theory became an equivalent discipline in physics, often preceding experimental achievements, and has remained in this position until to date. At the verge of the 21st century, a similar scenario appears to happen in chemistry, although for different reasons. While it was the appearance of fundamentally new theories and their consequences, giving theoretical research its powerful position in physics, in chemistry the general theoretical framework has been known since the work of Erwin Schrödinger, although substantially amplified and supplemented by his colleagues in the following decades. The driving force pushing theoretical work to its present position—and most probably improving this position continuously—was and is the methodical development of numerical solutions and the technical progress of electronic computing. If nowadays a large amount of chemical research cannot be performed at a state-of-the-art level without the inclusion of theory experts, and computational chemistry can give answers to problems experimentally unaccessible, it has to be credited to these developments. It seems justified, therefore, to state that we are witnessing a "computational revolution" of chemistry, which will not only influence scientific research and modernize teaching curricula, but increasingly industrial chemistry as well.

SUPPORTING MATERIALS

Video clips of recent simulations are available for download at <www.molvision.com>, section "Video Clips":

1. Cu(II) in water
2. Cu(II) mono-amine complex in water
3. Cu(II) *cis*-diamine complex in water
4. Cu(II) *trans*-diamine complex in water
5. Water
6. Au(I) in water
7. Cs(I) in water
8. Cu(II) in liquid ammonia
9. Dynamics of oligopeptides in water
10. Ni(II)–NH_3 complexes in water
11. Dynamics of Na(I) and K(I) in water
12. Dynamics of fluoride and chloride ions in water

ACKNOWLEDGMENT

Support of this work by the Austrian Science Foundation (Project 16221) is gratefully acknowledged.

REFERENCES AND NOTES

1. E. Schrödinger. *Ann. Phys*. **79**, 361 (1926).
2. M. J. Elrod, R. J. Saykelly. *Chem. Rev*. **94**, 1974 (1994).
3. B. M. Rode, C. F. Schwenk, A. Tongraar. *J. Mol. Liq.* **110**, 105 (2003).
4. B. M. Rode, C. F. Schwenk, T. S. Hofer, B. R. Randolf. *Coord. Chem. Rev.* **249**, 2993 (2005).
5. G. W. Marini, K. R. Liedl, B. M. Rode. *J. Phys. Chem. A* **103**, 11387 (1999).
6. G. W. Marini, N. R. Texler, B. M. Rode. *J. Phys. Chem*. **100**, 6808 (1996).
7. J. Brodholt, M. Sampoli, R. Vallauri. *Mol. Phys*. **86**, 149 (1995).
8. A. A. Chialvo, P. T. Cummings. *J. Chem. Phys.* **105**, 8274 (1996).
9. L. X. Dang, T. M. Chang. *J. Chem. Phys*. **106**, 8149 (1997).
10. M. P. Allen, D. J. Tildesley. *Computer Simulation of Liquids*, Oxford Science Publications, Oxford (1990).
11. N. Metropolis, A. W. Rosenbluth, M. N. Rosenbluth, A. H. Teller, E. Teller. *J. Chem. Phys.* **21**, 1087 (1953).
12. H. J. C. Berendsen, J. P. M. Postma, W. F. van Gunsteren, A. DiNola, J. R. Haak. *J. Phys. Chem.* **81**, 3684 (1984).
13. A. Warshel, M. Levitt. *J. Mol. Biol*. **103**, 227 (1976).
14. M. J. Field, P. A. Bash, M. Karplus. *J. Comput. Chem.* **11**, 700 (1990).
15. J. Gao. *J. Am. Chem. Soc.* **115**, 2930 (1993).
16. D. Bakowies, W. Thiel. *J. Phys. Chem*. **100**, 10580 (1996).
17. E. F. H. Michael, J. S. Dewar, E. G. Zoebisch, J. J. P. Stewart. *J. Am. Chem. Soc*. **107**, 3902 (1985).
18. J. J. P. Stewart. *J. Comput. Chem*. **10**, 209 (1989).
19. T. Kerdcharoen, K. R. Liedl, B. M. Rode. *Chem. Phys*. **211**, 313 (1996).
20. A. D. Becke. *Phys. Rev*. **38**, 3098 (1988).
21. C. Lee, W. Yang, R. G. Parr. *Phys. Rev. B* **37**, 785 (1988).
22. R. Car, M. Parinello. *Phys. Rev. Lett*. **55**, 2471 (1985).

23. A. Pasquarello, I. Petri, P. S. Salmon, O. Parisel, R. Car, É. Tóth, D. H. Powell, H. E. Fischer, L. Helm, A. Merbach. *Science* **291**, 856 (2001).
24. I. Bákо, J. Hutter, G. G. Pálinkás. *J. Chem. Phys*. **117**, 9838 (2002).
25. C. F. Schwenk, B. M. Rode. *J. Chem. Phys*. **119**, 9523 (2003).
26. A. D. Becke. *J. Chem. Phys*. **98**, 5648 (1993).
27. C. F. Schwenk, T. S. Hofer, B. M. Rode. *J. Phys. Chem. A* **108**, 1509 (2004).
28. C. F. Schwenk, H. H. Löffler, B. M. Rode. *J. Chem. Phys*. **115**, 10808 (2001).
29. T. S. Hofer, H. T. Tran, C. F. Schwenk, B. M. Rode. *J. Comput. Chem*. **25**, 211 (2004).
30. H. Erras-Hanauer, T. Clark, R. van Eldik. *Coord. Chem. Rev*. **238–239**, 233 (2003).
31. C. F. Schwenk, M. J. Loferer, B. M. Rode. *Chem. Phys. Lett*. **382**, 460 (2003).
32. G. W. Neilson, A. K. Adya. *Ann. Rep. Chem., Sect. C* **93**, 101 (1996).
33. G. W. Neilson, P. E. Mason, S. Ramos, D. Sullivan. *Philos. Trans. R. Soc. London, Ser. A* **359**, 1575 (2001).
34. A. Tongraar, K. Sagarik, B. M. Rode. *Phys. Chem. Chem. Phys*. **4**, 628 (2002).
35. R. R. Pappalardo, E. S. Marcos. *J. Phys. Chem*. **97**, 4500 (1993).
36. H. Saint-Martin, C. Medina-Llanos, I. Ortega-Blake. *J. Chem. Phys.* **93**, 6448 (1990).
37. F. H. Stillinger, A. Rahman. *J. Chem. Phys*. **68**, 666 (1978).
38. P. Bopp, G. Janscó, K. Heinzinger. *Chem. Phys. Lett*. **98**, 129 (1983).
39. R. Ahlrichs, M. Bär, M. Häser, H. Horn, C. Kölmel. *Chem. Phys. Lett*. **162**, 165 (1989).
40. S. Brode, H. Horn, M. Ehrig, D. Moldrup, J. E. Rice, R. Ahlrichs. *J. Comput. Chem*. **14**, 1142 (1993).
41. R. Ahlrichs, M. von Arnim. In *TURBOMOLE, Parallel Implementation of SCF, Density Functional, and Chemical Shift Modules*, E. Clementi, G. Corongiu (Eds.), Chap. 13, pp. 509–554, STEF, Cagliari (1995).
42. M. von Arnim, R. Ahlrichs. *J. Comput. Chem*. **19**, 1746 (1998).
43. A. J. Lock, S. Woutersen, H. J. Bakker. *Femtochemistry and Femtobiology*, World Scientific, Singapore (2001).
44. H. T. Tran, B. M. Rode. <http://www.molvision.com> (unpublished).
45. A. Wallqvist, R. D. Mountain. *Rev. Comput. Chem.* **13**, 183 (1999).
46. B. Guillot. *J. Mol. Liq*. **101**, 219 (2002).
47. A. K. Soper. *J. Phys.: Condens. Matter* **9**, 2717 (1997).
48. E. Clementi, G. Corongui. *Int. J. Quantum Chem., Symp*. **10**, 31 (1983).
49. J. H. Detrich, E. Clementi, G. Corongui. *Chem. Phys. Lett.* **112**, 426 (1984).
50. L. A. Curtiss, J. W. Halley, J. Hautman, A. Rahman. *J. Chem. Phys.* **86**, 2319 (1987).
51. P. Wernet, D. Nordlund, U. Bergmann, M. Cavalleri, M. Odelius, H. Ogasawara, L. A. Näslund, T. K. Hirsch, L. Ojamäe, P. Glatzel, L. G. M. Pettersson, A. Nilsson. *Science* **304**, 955 (2004).
52. J. B. R. Bucher, J. Stauber. *Chem. Phys. Lett*. **306**, 57 (1999).
53. D. Xenides, B. R. Randolf, B. M. Rode. *J. Chem. Phys*. **122**, 4506 (2005).
54. C. F. Schwenk, B. M. Rode. *J. Am. Chem. Soc.* **126**, 12786 (2004).
55. C. F. Schwenk, T. S. Hofer, B. M. Rode. *J. Phys. Chem. A* **108**, 1509 (2004).
56. C. F. Schwenk, B. M. Rode. *J. Chem. Phys*. **119**, 9523 (2003).
57. R. Leberman, A. K. Soper. *Nature* **378**, 364 (1995).
58. H. A. Jahn, E. Teller. *Proc. R. Soc. London, Ser. A* **161**, 220 (1937).
59. L. Curtiss, J. W. Halley, X. R. Wang. *Phys. Rev. Lett*. **69**, 2435 (1992).
60. I. Persson, P. Persson, M. Sandström, A.-S. Ullström. *J. Chem. Soc., Dalton Trans.* **7**, 1256 (2002).
61. A. Neubrand, F. Thaler, M. Krner, A. Zahl, C. D. Hubbard, R. van Eldik. *J. Chem. Soc., Dalton Trans.* **6**, 957 (2002).
62. J. J. Blumberger, L. Bernasconi, I. Tavernelli, R. Vuilleumier, M. Sprik. *J. Am. Chem. Soc.* **126**, 3928 (2004).

63. D. H. Powell, L. Helm, A. E. Merbach. *J. Chem. Phys*. **95**, 9258 (1991).
64. C. Kritayakornupong, K. Plankensteiner, B. M. Rode. *ChemPhysChem* **5**, 1499 (2004).
65. H. Ohtaki, T. Radnai. *Chem. Rev*. **93**, 1157 (1993).
66. T. S. Hofer, A. B. Pribil, B. R. Randolf, B. M. Rode. *J. Am. Chem. Soc*. **127**, 14231 (2005).
67. T. S. Hofer, B. M. Rode. *J. Chem. Phys*. **121**, 6406 (2004).
68. C. Kritayakornupong, K. Plankensteiner, B. M. Rode. *J. Comput. Chem*. **25**, 1576 (2004).
69. J. M. Martínez, R. R. Pappalardo, S. E. Marcos, K. Refson, S. D. A. Munoz-Paez. *J. Phys. Chem. B* **102**, 3272 (1998).
70. J. M. Martínez, R. R. Pappalardo, E. S. Marcos. *J. Chem. Phys*. **109**, 1445 (1998).
71. T. S. Hofer, B. R. Randolf, B. M. Rode. *Phys. Chem. Chem. Phys*. **7**, 1382 (2005).
72. J. M. Martínez, R. R. Pappalardo, E. S. Marcos. *J. Am. Chem. Soc*. **121**, 3175 (1999).
73. D. Spångberg, K. Hermansson. *J. Chem. Phys.* **120**, 4829 (2004).
74. E. Wasserman, J. R. Rustad, S. S. Xantheas. *J. Chem. Phys*. **106**, 9769 (1997).
75. R. Armunanto, C. F. Schwenk, B. M. Rode. *J. Phys. Chem. A* **107**, 3132 (2003).
76. A. Tongraar, K. R. Liedl, B. M. Rode. *J. Phys. Chem. A* **102**, 10340 (1998).
77. A. Tongraar, B. M. Rode. *Chem. Phys. Lett.* **385**, 378 (2004).
78. C. Kritayakornupong, K. Plankensteiner, B. M. Rode. *Chem. Phys. Lett.* **371**, 438 (2003).
79. R. Armunanto, C. F. Schwenk, B. R. Randolf, B. M. Rode. *Chem. Phys. Lett.* **388**, 395 (2004).
80. R. Armunanto, C. F. Schwenk, B. M. Rode. *J. Am. Chem. Soc*. **126**, 9934 (2004).
81. C. H. Langford, H. B. Gray. *Ligand Substitution Processes*, W. A. Benjamin, New York (1965).
82. L. Helm, A. E. Merbach. *Coord. Chem. Rev.* **187**, 151 (1999).
83. L. Helm, A. E. Merbach. *Chem. Rev*. **105**, 1923 (2005).
84. C. J. Cramer, D. G. Truhlar. *Chem. Rev*. **99**, 2161 (1999).
85. F. P. Rotzinger. *Chem. Rev*. **105**, 2003 (2005).
86. C. F. Schwenk, B. M. Rode. *Phys. Chem. Chem. Phys.* **5**, 3418 (2003).
87. C. F. Schwenk, T. S. Hofer, B. R. Randolf, B. M. Rode. *Phys. Chem. Chem. Phys*. **7**, 1669 (2005).
88. A. Tongraar, K. R. Liedl, B. M. Rode. *Chem. Phys. Lett.* **286**, 56 (1998).
89. T. S. Hofer, B. R. Randolf, B. M. Rode. *J. Comput. Chem.* **26**, 949 (2005).
90. R. Armunanto, C. F. Schwenk, H. T. Tran, B. M. Rode. *J. Am. Chem. Soc*. **126**, 2582 (2004).
91. A. Tongraar, K. Sagarik, B. M. Rode. *J. Phys. Chem. B* **105**, 10559 (2001).
92. A. Tongraar, B. M. Rode. *Chem. Phys. Lett*. **409**, 304 (2005).
93. B. M. Rode, T. S. Hofer. Unpublished results.
94. T. S. Hofer, B. M. Rode, B. R. Randolf. *Chem. Phys.* **312**, 81 (2005).
95. C. F. Schwenk, H. H. Loeffler, B. M. Rode. *J. Am. Chem. Soc*. **125**, 1618 (2003).
96. T. Remsungnen, B. M. Rode. *J. Phys. Chem. A* **107**, 2324 (2003).
97. R. Armunanto, C. F. Schwenk, A. H. Setiaji, B. M. Rode. *Chem. Phys*. **295**, 63 (2003).
98. M. Q. Fatmi, T. S. Hofer, B. R. Randolf, B. M. Rode. *J. Chem. Phys*. **123**, 4514 (2005).
99. C. Kritayakornupong, K. Plankensteiner, B. M. Rode. *J. Phys. Chem. A* **107**, 10330 (2003).
100. C. Kritayakornupong, K. Plankensteiner, B. M. Rode. *J. Phys. Chem.* **119**, 6068 (2003).
101. B. J. Palmer, D. M. Pfund, J. L. Fulton. *J. Phys. Chem*. **100**, 13393 (1996).
102. A. Filipponia, P. D'Angelo, N. V. Pavel, A. Di Cicco. *Chem. Phys. Lett.* **225**, 150 (1994).
103. P. J. Merkling, A. Muñoz-Páez, R. R. Pappalardo, E. S. Marcos. *Phys. Rev. B* **64**, 2201 (2001).
104. S. Della Longa, A. Arcovito, M. Girasole, J. L. Hazemann, M. Benfatto. *Phys. Rev. Lett*. **87**, 5501 (2001).
105. A. J. Stone. *The Theory of Intermolecular Forces*, Oxford University Press, Oxford (1995).
106. B. M. Rode, T. S. Hofer, B. R. Randolf, C. F. Schwenk, D. Xenides, V. Vchirawongkwin. *Theor. Chem. Acc.* (2006). In press (DOI: 10.1007/s00214).